Supplement of Solid Earth, 14, 137–151, 2023
https://doi.org/10.5194/se-14-137-2023-supplement

Solid Earth
Open Access

Supplement of

Seismic amplitude response to internal heterogeneity of mass-transport deposits

Jonathan Ford et al.

Correspondence to: Jonathan Ford (jford@ogs.it)

Contents of this file

1. Black Sea case study area additional data:

   (a) Multi-sensor core logger (MSCL) data for four sediment cores (Fig. S1)

   (b) Cone penetration test (CPT) data for site GH-T-PCPT7 (Fig. S2)

   (c) Stacking velocity function from close to the alongslope sub-bottom profile (Fig. S3)

2. Synthetic modelling trace envelope results for all realisations:

   (a) Single-source experiment (Fig. S4)

   (b) Multi-source experiment (Fig. S5)

3. Model details and summary results for variations on the single-source synthetic experiment:

   (a) 'Low-reflectivity' experiment (Table S1 and Fig. S10)

   (b) 'High-reflectivity' experiment (Table S2 and Fig. S11)

   (c) 'Far source' experiment (Table S3, Figs. S12 and S13)

   (d) 'Low Poisson's ratio' experiment (Table S4 and Fig. S14)

   (e) Cross-plot between the single-source synthetic experiment and experiments (a) to (d) of RMS amplitudes within the heterogeneous zone (Fig. S15)

4. Compute requirements for the synthetic modelling experiments (Table S5)

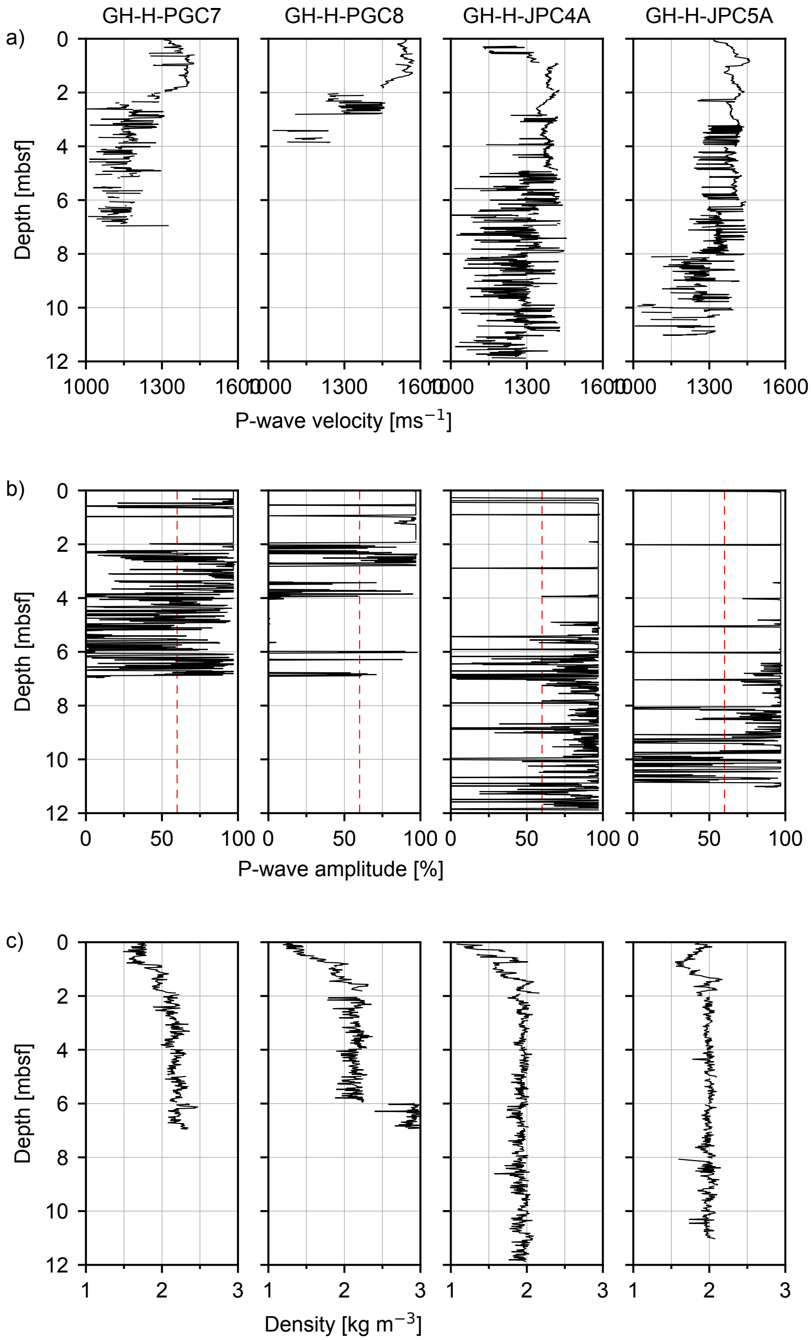

Figure S1. Multi-sensor core logger (MSCL) results from cores GH-H-PGC7, GH-H-PGC8, GH-H-JPC4A and GH-H-JPB5A. a) P-wave velocity, b) P-wave amplitude (60% cutoff marked), c) density, d) cross-plot of P-wave velocity and density logs, for depth intervals where the P-wave amplitude exceeds the 60% cutoff. Parameter distributions are used to derive geologically plausible P-impedance contrasts for the two component sediment lithologies used in the multi-source synthetic experiment (Section 3.2) (cont.)

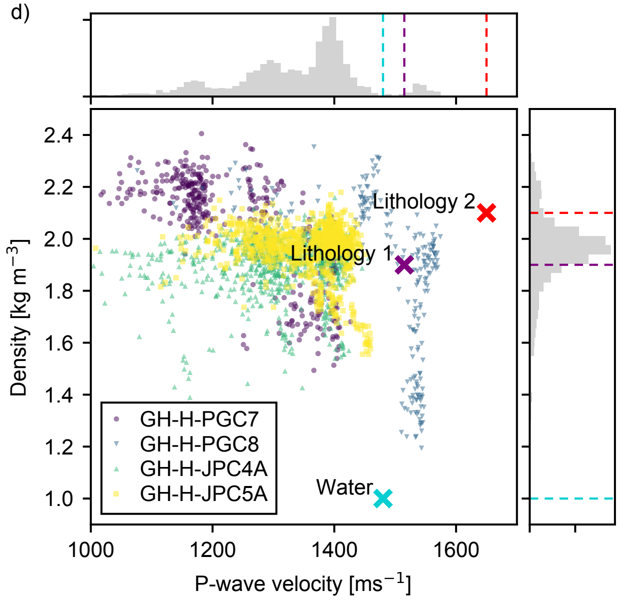
d)
Lithology 2
Lithology 1
Water
GH-H-PGC7
GH-H-PGC8
GH-H-JPC4A
GH-H-JPC5A
Density [kg m^{-3}]
P-wave velocity [ms^{-1}]
2.4
2.2
2.0
1.8
1.6
1.4
1.2
1.0
1000
1200
1400
1600

Figure S1.

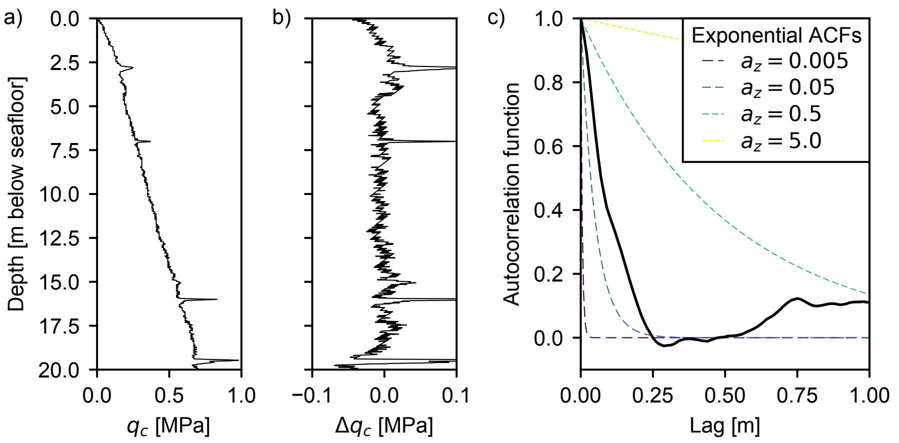

Figure S2. Cone-penetration test (CPT) results for site GH-T-PCPT7. a) Cone-tip resistance (q_c) log, b) De-trended cone-tip resistance log (Δq_c), de-trended with a best fit linear trend, c) Autocorrelation function (ACF) of the cone-tip resistance log.

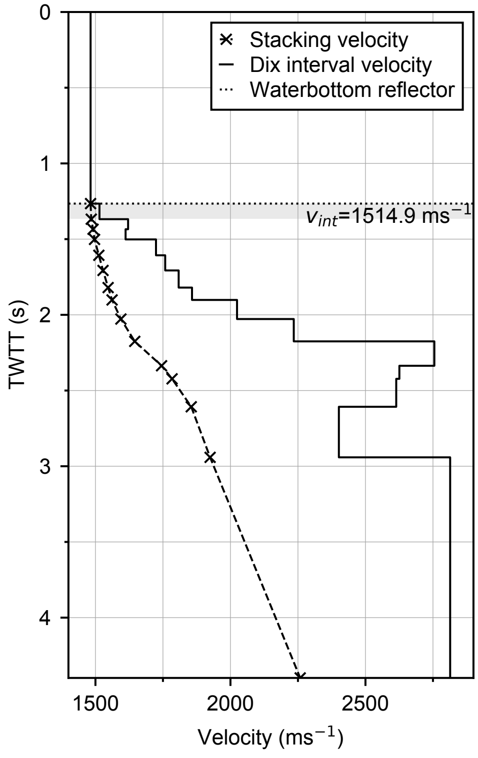

Figure S3. Picked NMO stacking velocities for a common mid-point gather from a multi-channel seismic reflection profile located close to the alongslope Black Sea sub-bottom profile (location in Fig. 1a). The water velocity is 1480 ms^{-1}, and the average Dix-converted interval velocity (v_{int}) for 100 ms beneath the seafloor (shaded grey) is marked. 'TWTT' corresponds to two-way traveltime.

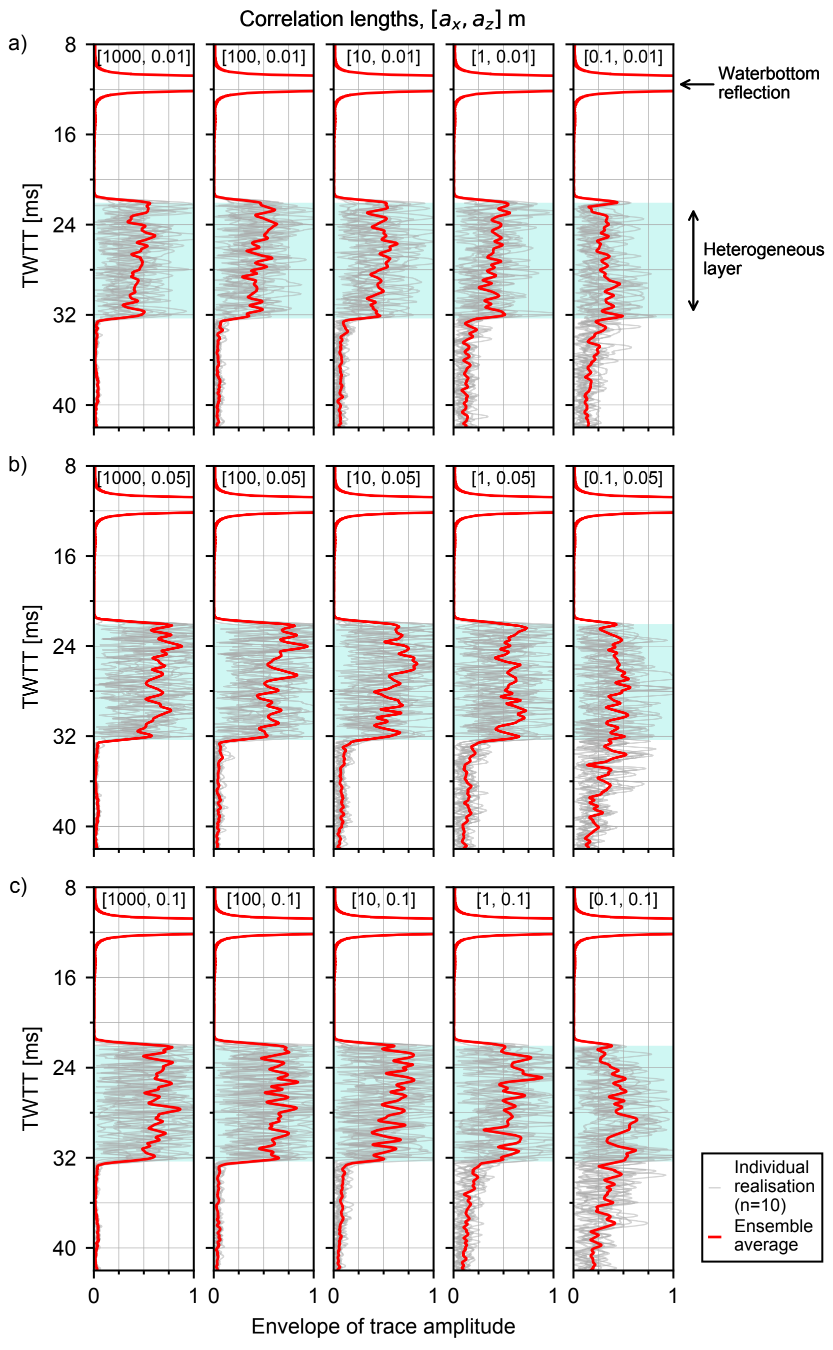

Figure S4. Envelope of trace amplitude for individual realisations (grey) and the RMS envelope of the single-source synthetic experiment for each unique set of correlation lengths (red) for a range of vertical correlation lengths $a_z = \{0.01, 0.05, 0.1, 0.5, 1\}$ m (a-e) and lateral correlation lengths $a_x = \{1000, 100, 10, 1, 0.1\}$ m (left to right). The two-way traveltime (TWTT) extent of the heterogeneous layer is shaded in blue. (cont.)

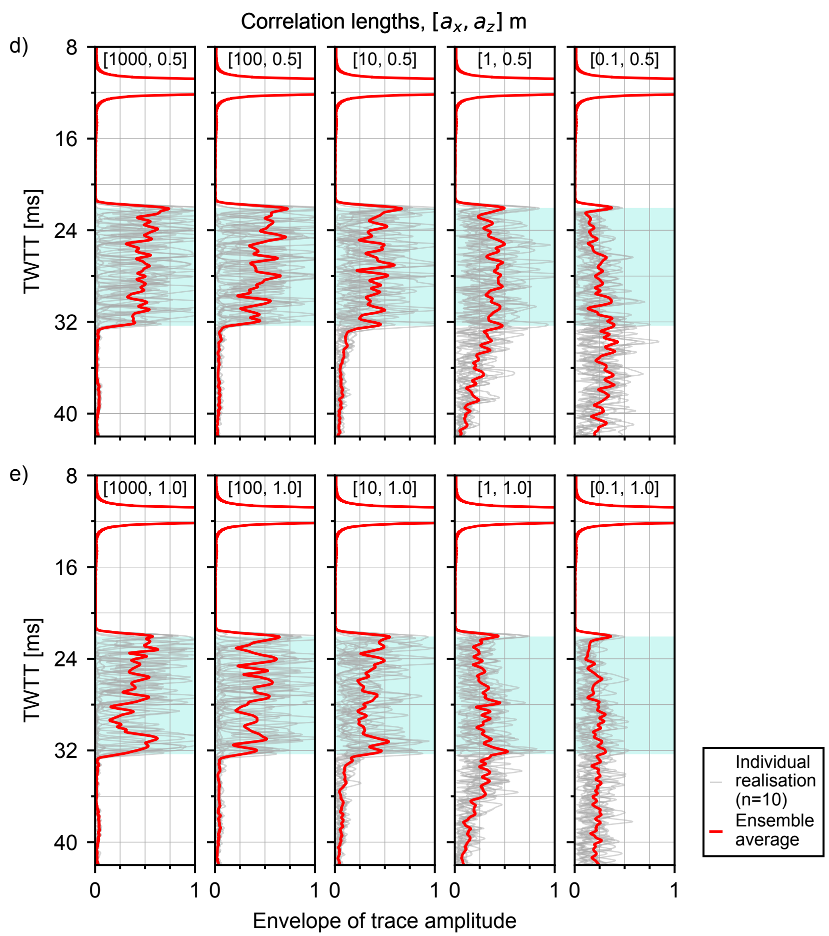
Correlation lengths, [a_x, a_z] m
d)
[1000, 0.5]
[100, 0.5]
[10, 0.5]
[1, 0.5]
[0.1, 0.5]
e)
[1000, 1.0]
[100, 1.0]
[10, 1.0]
[1, 1.0]
[0.1, 1.0]
TWTT [ms]
8
16
24
32
40
0
1
Envelope of trace amplitude
Individual realisation (n=10)
Ensemble average

Figure S4.

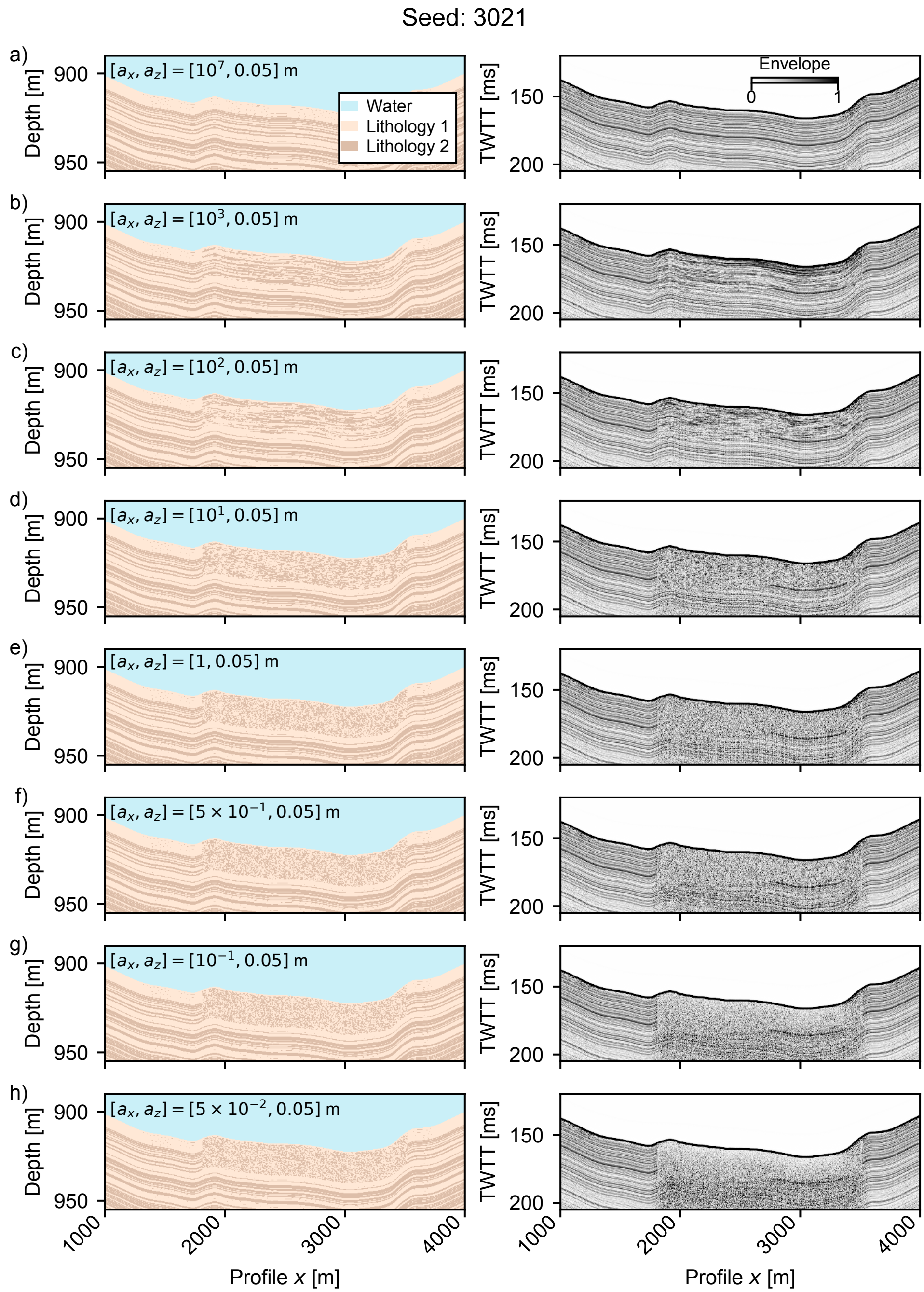

Figure S5. Realisations of the multi-source synthetic experiment models (left) and resulting synthetic sub-bottom profiles (right) for seed 3021, lateral scale lengths $a_x = \{1 \times 10^7(\text{unfailed}), 1000, 100, 10, 1, 0.5, 0.1, 0.05\}$ (a-h) and vertical scale length $a_z = 0.05$ m.

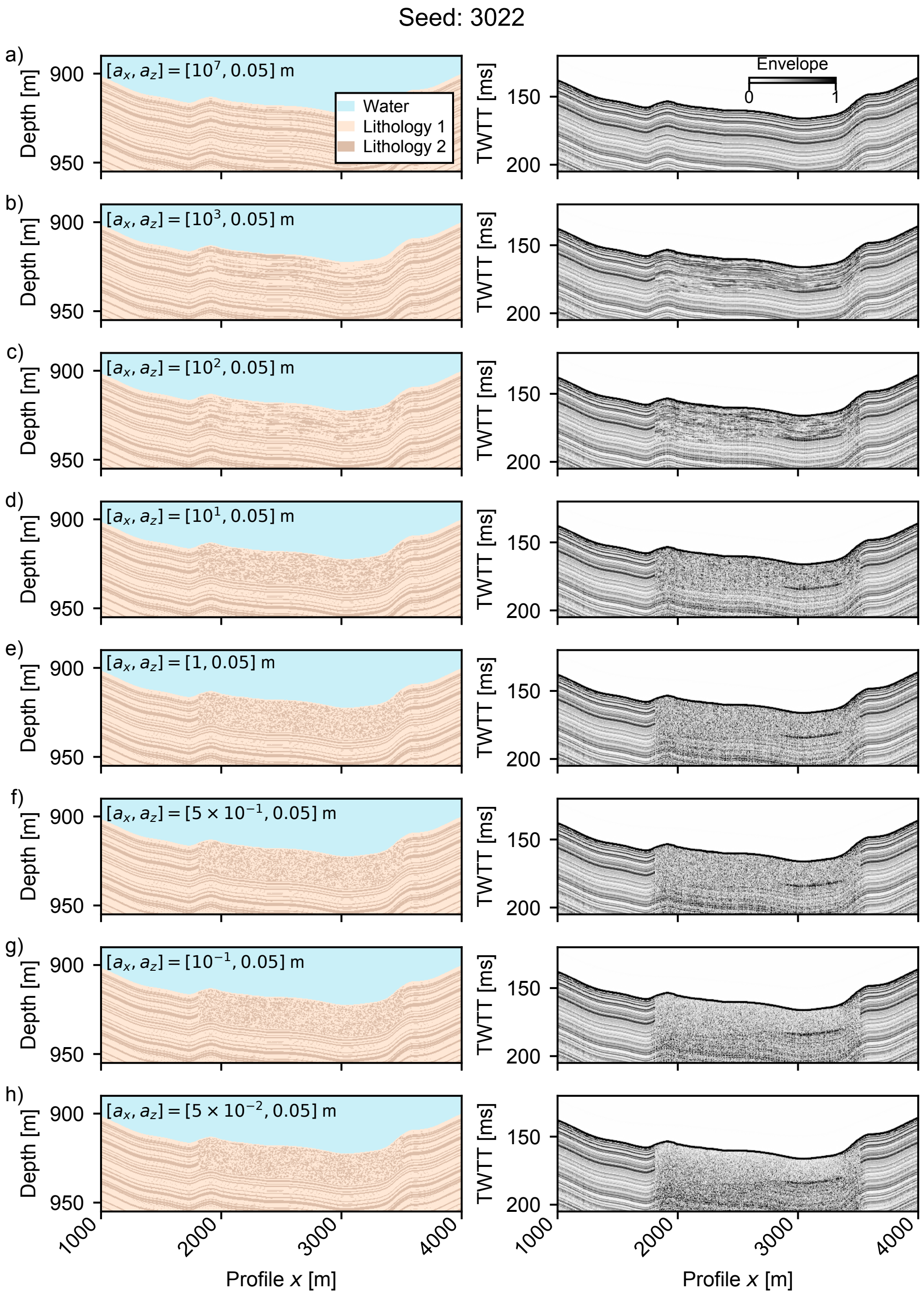

Figure S6. Realisations of the multi-source synthetic experiment models (left) and resulting synthetic sub-bottom profiles (right) for seed 3022, lateral scale lengths $a_x = \{1 \times 10^7 (\text{unfailed}), 1000, 100, 10, 1, 0.5, 0.1, 0.05\}$ (a-h) and vertical scale length $a_z = 0.05$ m.

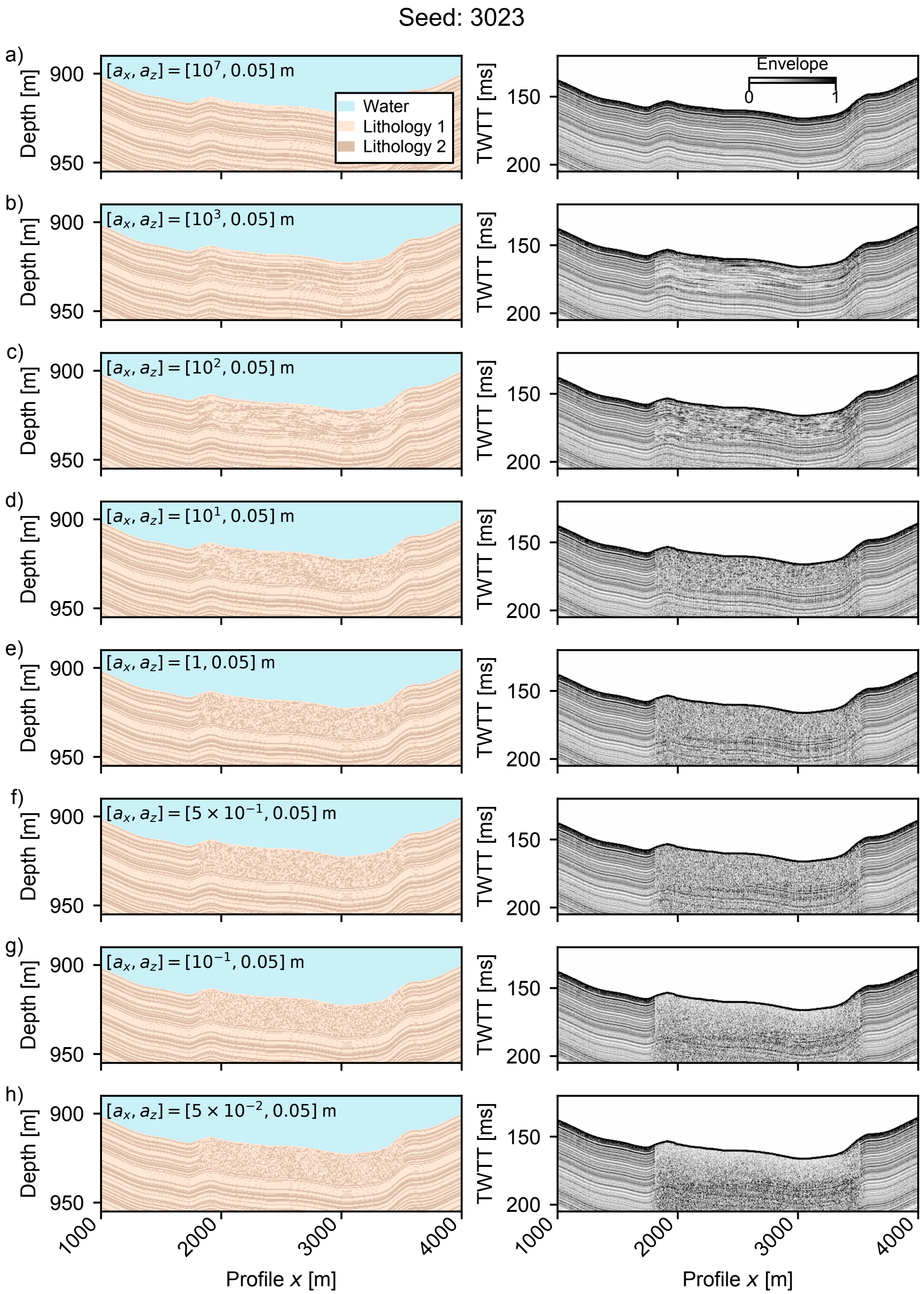

Figure S7. Realisations of the multi-source synthetic experiment models (left) and resulting synthetic sub-bottom profiles (right) for seed 3023, lateral scale lengths $a_x = \{1 \times 10^7(\text{unfailed}), 1000, 100, 10, 1, 0.5, 0.1, 0.05\}$ (a-h) and vertical scale length $a_z = 0.05$ m.

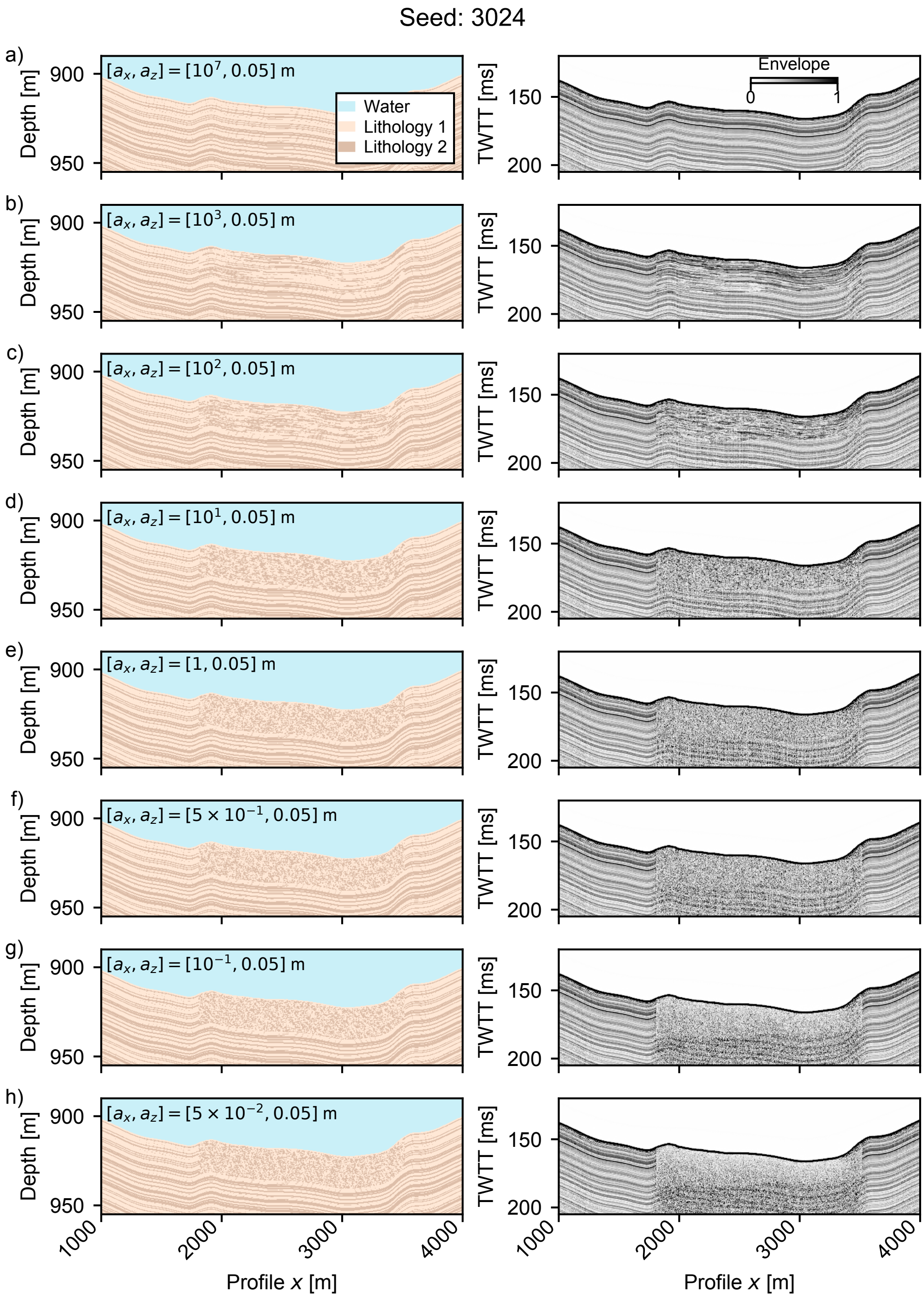

Figure S8. Realisations of the multi-source synthetic experiment models (left) and resulting synthetic sub-bottom profiles (right) for seed 3024, lateral scale lengths $a_x = \{1 \times 10^7(\text{unfailed}), 1000, 100, 10, 1, 0.5, 0.1, 0.05\}$ (a-h) and vertical scale length $a_z = 0.05$ m.

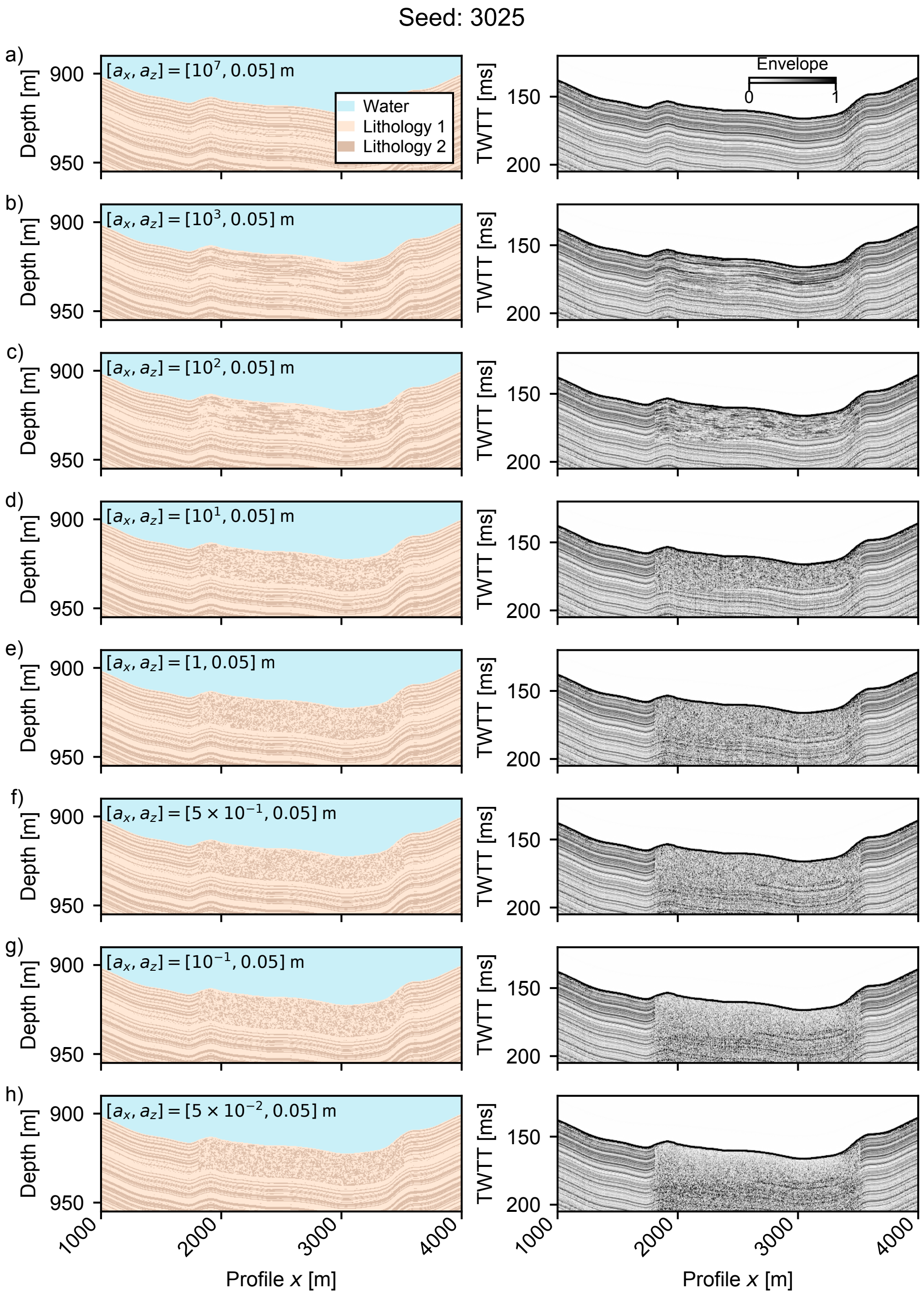

Figure S9. Realisations of the multi-source synthetic experiment models (left) and resulting synthetic sub-bottom profiles (right) for seed 3025, lateral scale lengths $a_x = \{1 \times 10^7(\text{unfailed}), 1000, 100, 10, 1, 0.5, 0.1, 0.05\}$ (a-h) and vertical scale length $a_z = 0.05$ m.

Table S1. Modelling parameters for the 'low reflectivity' single-source synthetic experiment, including the elastic parameters for the water layer and the two sediment lithologies. The model geometry is identical to the single-source experiment (Fig. 3).

Component lithologies	P-wave velocity	S-wave velocity	Density
Water	1480 ms^{-1}	—	1000 kgm^{-3}
Lithology 1	1515 ms^{-1}	379 ms^{-1}	1900 kgm^{-3}
Lithology 2	1550 ms^{-1}	388 ms^{-1}	1950 kgm^{-3}
Finite-difference modelling parameters			
Model dimensions	40×40 m (1601 $\times$ 1601 grid points)		
Grid spacing	0.025×0.025 m		
Timestep	0.0089 ms		
Modelling time	43.7 ms (4908 timesteps)		
Absorbing boundaries	Sponge layers on all four grid edges		
Source wavelet	1.5 kHz Ricker wavelet (zero-phase)		

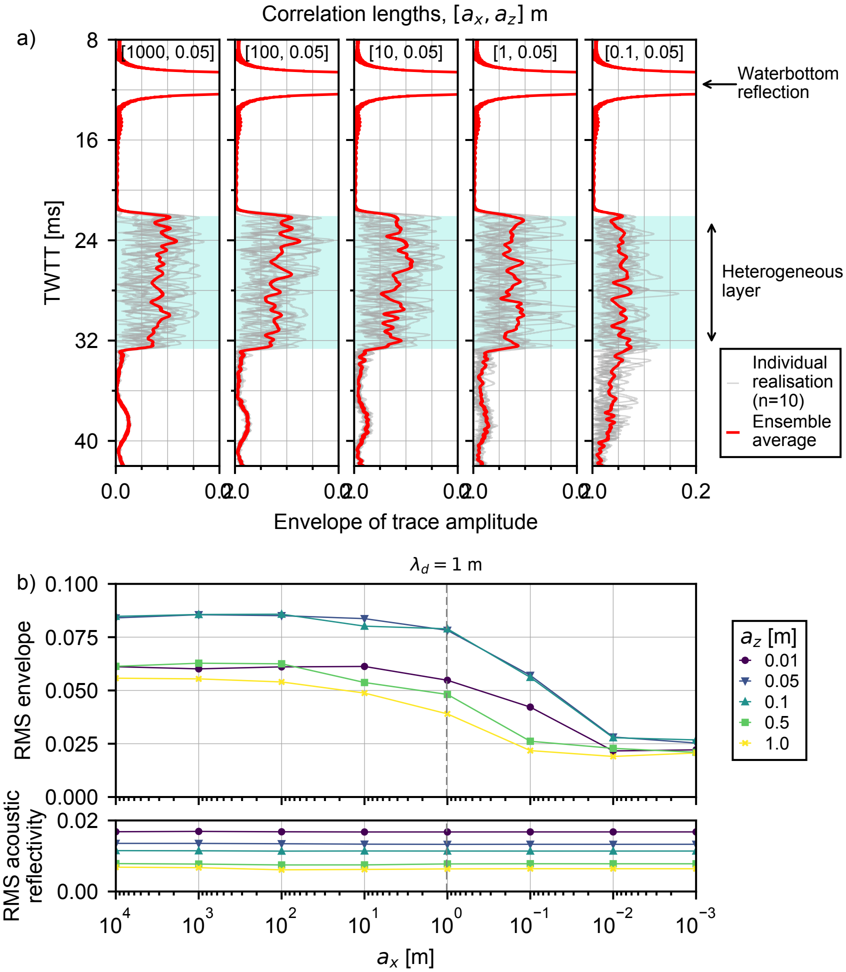

Figure S10. ‘Low reflectivity’ single-source synthetic experiment results. a) Envelope of trace amplitude for $n = 10$ multiple realisations (grey) and the RMS envelope of all realisations (red) for fixed vertical correlation length $a_z = 0.05$ m and lateral correlation lengths $a_x = \{1000, 100, 10, 1, 0.1\}$ m (from left to right). The two-way traveltime (TWTT) extent of the heterogeneous layer is shaded in blue. b) (Top) RMS envelope within the heterogeneous zone against lateral correlation length, a_x, grouped by vertical correlation length, a_z. (Bottom) RMS vertical incidence acoustic reflectivity within the heterogeneous zone. λ_d shows the dominant wavelength of the seismic source in the sediment layers. Modelling parameters are given in Table S1.

Table S2. Modelling parameters for the 'high reflectivity' single-source synthetic experiment, including the elastic parameters for the water layer and the two sediment lithologies. The model geometry is identical to the single-source experiment (Fig. 3).

Component lithologies	P-wave velocity	S-wave velocity	Density
Water	1480 $\mathrm{ms^{-1}}$	—	1000 $\mathrm{kgm^{-3}}$
Lithology 1	1515 $\mathrm{ms^{-1}}$	379 $\mathrm{ms^{-1}}$	1900 $\mathrm{kgm^{-3}}$
Lithology 2	1800 $\mathrm{ms^{-1}}$	450 $\mathrm{ms^{-1}}$	2400 $\mathrm{kgm^{-3}}$
Finite-difference modelling parameters			
Model dimensions	40×40 m (1601 $\times$ 1601 grid points)		
Grid spacing	0.025×0.025 m		
Timestep	0.0080 ms		
Modelling time	43.7 ms (5470 timesteps)		
Absorbing boundaries	Sponge layers on all four grid edges		
Source wavelet	1.5 kHz Ricker wavelet (zero-phase)		

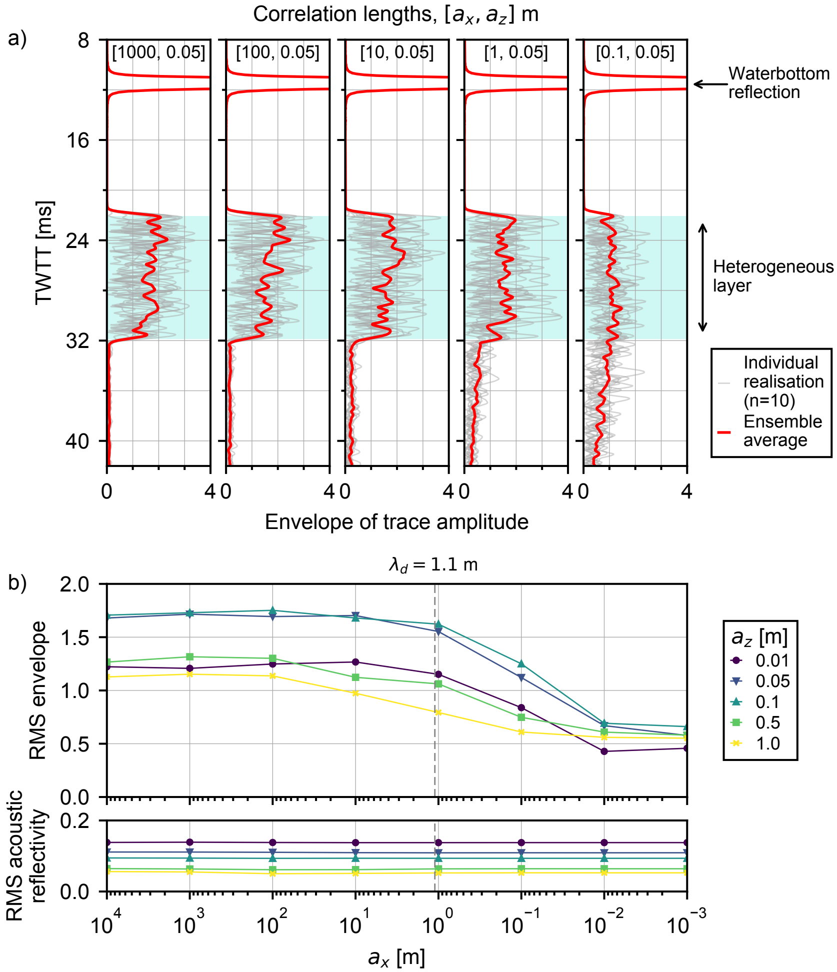

Figure S11. 'High reflectivity' single-source synthetic experiment results. a) Envelope of trace amplitude for $n = 10$ multiple realisations (grey) and the RMS envelope of all realisations (red) for fixed vertical correlation length $a_z = 0.05$ m and lateral correlation lengths $a_x = \{1000, 100, 10, 1, 0.1\}$ m (from left to right). The two-way traveltime (TWTT) extent of the heterogeneous layer is shaded in blue. b) (Top) RMS envelope within the heterogeneous zone against lateral correlation length, a_x, grouped by vertical correlation length, a_z. (Bottom) RMS vertical incidence acoustic reflectivity within the heterogeneous zone. λ_d shows the dominant wavelength of the seismic source in the sediment layers. Modelling parameters are given in Table S2.

Table S3. Modelling parameters for the 'far source' single-source synthetic experiment, including the elastic parameters for the water layer and the two sediment lithologies.

Component lithologies	P-wave velocity	S-wave velocity	Density
Water	1480 ms^{-1}	—	1000 kgm^{-3}
Lithology 1	1515 ms^{-1}	379 ms^{-1}	1900 kgm^{-3}
Lithology 2	1650 ms^{-1}	413 ms^{-1}	2100 kgm^{-3}
Finite-difference modelling parameters			
Model dimensions	80 × 80 m (3201 × 3201 grid points)		
Grid spacing	0.025 × 0.025 m		
Timestep	0.0089 ms		
Modelling time	97.0 ms (10915 timesteps)		
Seismic source	1.5 kHz Ricker wavelet (zero-phase)		

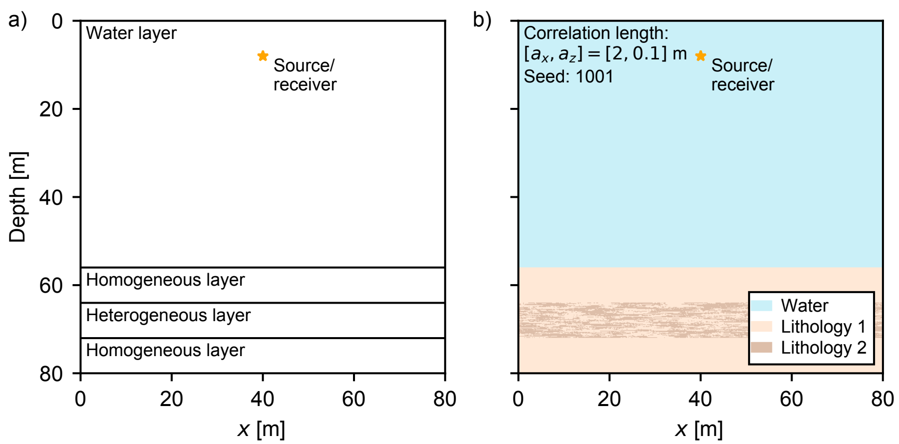

Figure S12. 'Far source' single-source synthetic experiment. a) Model geometry. The coincident seismic source and receiver (yellow star) is located within the water layer, 56 m from the top of the heterogeneous layer. b) A single realisation of the model showing the spatial distribution of Lithology 1 and Lithology 2 within the heterogeneous layer. Modelling parameters are listed in Table S3.

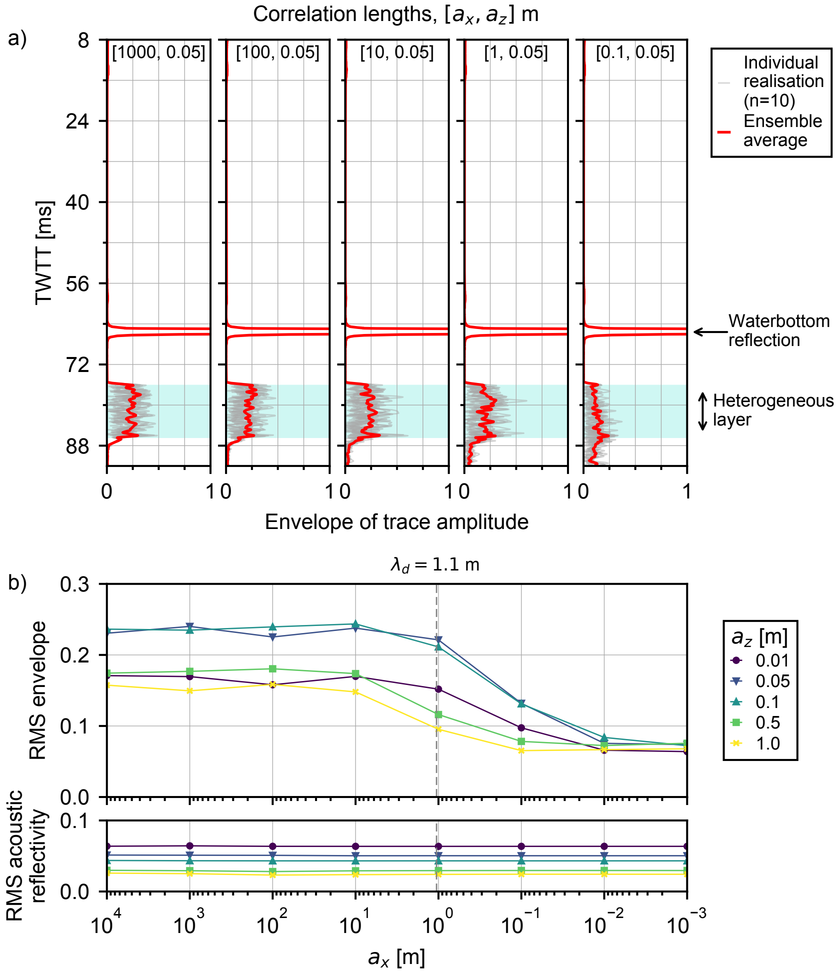

Figure S13. 'Far source' single-source synthetic experiment results. a) Envelope of trace amplitude for $n = 10$ multiple realisations (grey) and the RMS envelope of all realisations (red) for fixed vertical correlation length $a_z = 0.05$ m and lateral correlation lengths $a_x = \{1000, 100, 10, 1, 0.1\}$ m (from left to right). The two-way traveltime (TWTT) extent of the heterogeneous layer is shaded in blue. b) (Top) RMS envelope within the heterogeneous zone against lateral correlation length, a_x, grouped by vertical correlation length, a_z. (Bottom) RMS vertical incidence acoustic reflectivity within the heterogeneous zone. λ_d shows the dominant wavelength of the seismic source in the sediment layers. Modelling parameters are given in Table S3 and the model geometry is shown in Fig. S12.

Table S4. Modelling parameters for the 'low Poisson's ratio' single-source synthetic experiment, including the elastic parameters for the water layer and the two sediment lithologies. Poisson's ratio $\nu = 0.33$ in the sediment layers, corresponding to $v_P/v_S = 2$.

Component lithologies	P-wave velocity	S-wave velocity	Density
Water	1480 ms^{-1}	—	1000 kgm^{-3}
Lithology 1	1515 ms^{-1}	758 ms^{-1}	1900 kgm^{-3}
Lithology 2	1650 ms^{-1}	825 ms^{-1}	2100 kgm^{-3}
Finite-difference modelling parameters			
Model dimensions	40×40 m (1601 $\times$ 1601 grid points)		
Grid spacing	0.025×0.025 m		
Timestep	0.0081 ms		
Modelling time	43.7 ms (5401 timesteps)		
Absorbing boundaries	Sponge layers on all four grid edges		
Source wavelet	1.5 kHz Ricker wavelet (zero-phase)		

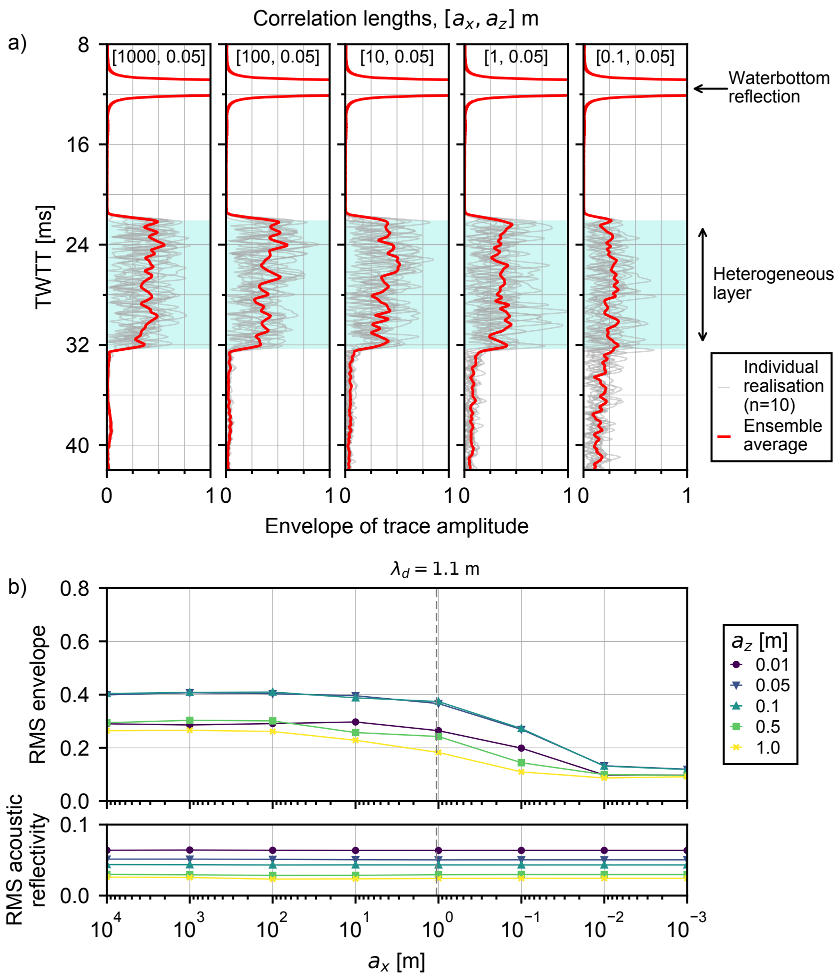

Figure S14. 'Low Poisson's ratio' single-source synthetic experiment results, where $\nu = 0.33$ in the sediment layers. a) Envelope of trace amplitude for $n = 10$ multiple realisations (grey) and the RMS envelope of all realisations (red) for fixed vertical correlation length $a_z = 0.05$ m and lateral correlation lengths $a_x = \{1000, 100, 10, 1, 0.1\}$ m (from left to right). The two-way traveltime (TWTT) extent of the heterogeneous layer is shaded in blue. b) (Top) RMS envelope within the heterogeneous zone against lateral correlation length, a_x, grouped by vertical correlation length, a_z. (Bottom) RMS vertical incidence acoustic reflectivity within the heterogeneous zone. λ_d shows the dominant wavelength of the seismic source in the sediment layers. Modelling parameters are given in Table S4.

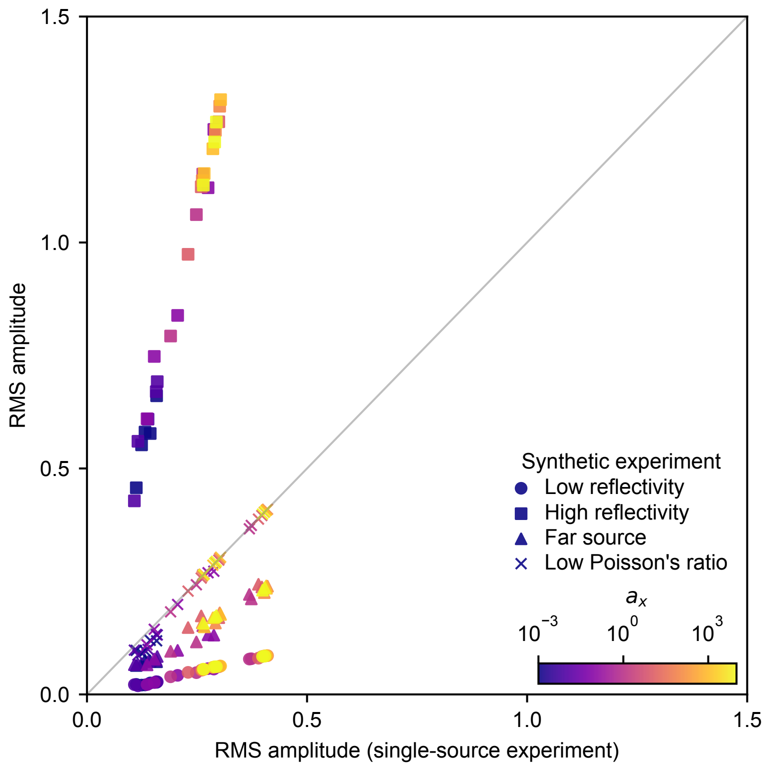

Figure S15. Cross-plot of the average RMS amplitudes within the heterogeneous zone, between the single-source experiment (Fig. 4) and the 'low reflectivity' (Fig. S10), 'high reflectivity' (Fig. S11), 'far source' (Fig. S13) and 'low Poisson's ratio' (Fig. S14) synthetic experiments.

Table S5. Approximate computational runtimes for the single-source and multi-source experiments. Models were run on an HPC cluster with 48-core nodes (2 × 24-core Intel Xeon Platinum 8276-8276L) and 384 GB memory. Quoted CPU times are per logical CPU core. For the multi-source experiment, the runtime of each shot represents the average computation time for each sub-model, as the exact sub-model grid size depends on the source location within the global model (Section 3.2). Modelling runs for sub-models that are identical with changing a_x (i.e., sub-models that do not overlap the MTD zone) are re-used, resulting in approximately 30% reduction in compute time compared to modelling all sub-models.

Synthetic experiment	CPU time (single shot)	Number of shots	CPU time (total)
Single-source 'Low reflectivity' 'High reflectivity' 'Low Poisson's ratio'	12 mins	400	80 hours
'Far source' single-source	1 hour	400	420 hours
Multi-source	10 mins	37 224 modelled (+ 22 816 cached shots)	6 200 hours